

**Frédéric Dumestre,<sup>a</sup> Brigitte Soula,<sup>a</sup> Anne-Marie Galibert,<sup>a</sup> Paul-Louis Fabre,<sup>\*a</sup>  
Gérald Bernardinelli,<sup>b</sup> Bruno Donnadieu<sup>c</sup> and Paule Castan<sup>a</sup>**

<sup>c</sup> Laboratoire de Chimie de Coordination, UPR CNRS 8241, 205 route de Narbonne, 31077 Toulouse, France

*J. Chem. Soc., Dalton Trans.*, 1998, 4131–4137      **4131**

**Table 1** Summary of crystal data, intensity measurements and structure refinement for [CoL<sup>1</sup>(H<sub>2</sub>O)<sub>3</sub>] **1** and K<sub>2</sub>[CoL<sub>2</sub>(H<sub>2</sub>O)<sub>2</sub>]**2**·2H<sub>2</sub>O **2**

Compound	<b>1</b>	<b>2</b>
Formula	[Co(C <sub>5</sub> O <sub>8</sub> )(H <sub>2</sub> O) <sub>3</sub> ] <sub>n</sub>	[K <sub>2</sub> Co(C <sub>11</sub> N <sub>4</sub> O <sub>3</sub> ) <sub>2</sub> (H <sub>2</sub> O) <sub>4</sub> ] <sub>0.5</sub>
Color	Purple	Red-brown
<i>M</i>	253.0	340.7
Crystal system	Orthorhombic	Monoclinic
Space group	<i>Pbca</i>	<i>P2<sub>1</sub>/n</i>
<i>a</i> /Å	11.869(2)	10.4257(7)
<i>b</i> /Å	8.114(2)	10.7946(6)
<i>c</i> /Å	15.393(3)	11.7045(6)
$\beta$ /°		108.726(3)
<i>U</i> /Å <sup>3</sup>	1482.5(2)	1247.5(1)
<i>Z</i>	8	4
<i>D<sub>c</sub></i> /g cm <sup>-3</sup>	2.267	1.881
<i>A</i> <sup>*</sup> <sub>min</sub> , <i>A</i> <sup>*</sup> <sub>max</sub>	3.897, 6.277	3.398, 6.585
<i>F</i> (000)	1019	682
$\mu$ /mm <sup>-1</sup>	2.33	9.075
<i>hkl</i> Ranges	0 to 13, 0 to 9, 0 to 17	−10 to 10, 0 to 11, 0 to 12
<i>T</i> /K	180	200
Scan range, $2\theta$ /°	2.9–48.4	2–110
No. measured reflections	9095	1616
No. independent reflections	1128	1528
No. observed reflections	951 ( $[ F_o  \geq \sigma(F_o)]$ )	1315 ( $[ F_o  \geq 4\sigma(F_o)]$ )
No. parameters	152	209
Weighting scheme, $\omega$	Chebyshev	$1/[\sigma^2(F_o) + 0.0005(F_o^2)]$
Max. and min. $\Delta F/e$ Å <sup>-3</sup>	1.35, 0.87	0.64, 0.44
Goodness of fit <i>S</i>	1.01	2.35
<i>R</i> , <i>R<sub>w</sub></i>	0.051, 0.064	0.035, 0.040

(H<sub>2</sub>L<sup>1</sup>), its potassium salt (K<sub>2</sub>L<sup>1</sup>) and the potassium salt of croconate violet (K<sub>2</sub>L<sup>2</sup>) were prepared according to the procedures described by Fatiadi.<sup>14,15,24</sup> IR spectra were recorded on a Perkin-Elmer 983 G spectrometer coupled with a Perkin-Elmer infrared data station. Samples were run in the solid state in nujol mulls. UV/VIS spectra were registered on a Roucaire Shimadzu UV-3100 spectrophotometer in DMF at concentrations from 10<sup>-5</sup> to 10<sup>-6</sup> mol L<sup>-1</sup>. Magnetic susceptibility measurements, in the 4–300 K temperature range were carried out on polycrystalline samples with a Faraday-type magnetometer equipped with a continuous-flow Oxford Instruments cryostat. HgCo(NCS)<sub>4</sub> was used as a calibrant (susceptibility at 20 °C, 16.44 × 10<sup>-6</sup> cm<sup>3</sup> mol<sup>-1</sup>). The molar susceptibilities were corrected for ligand diamagnetism using Pascal's constants.<sup>25</sup> The corrections were estimated at −236 × 10<sup>-6</sup> and −270 × 10<sup>-6</sup> cm<sup>3</sup> mol<sup>-1</sup> for **1** [CoL<sup>1</sup>(H<sub>2</sub>O)<sub>3</sub>] and **2** K<sub>2</sub>[CoL<sub>2</sub>(H<sub>2</sub>O)<sub>2</sub>]**2**·2H<sub>2</sub>O respectively.

Electrochemical measurements were carried out with a home-made potentiostat or an Autolab (EcoChemie) controlled by a PC at room temperature. The electrochemical cell (10 cm<sup>3</sup>) was a conventional one with three electrodes: working electrode, Pt (diameter 2 mm, EDI Tacussel) for rotating disc electrode experiments (LSV, linear sweep voltammetry) and Pt (disc diameter 0.5 mm) for cyclic voltammetry experiments (CV); counter electrode, Pt wire; and reference electrode, double junction SCE. The experiments were carried out in DMF–Bu<sub>4</sub>NPF<sub>6</sub> 0.1 mol L<sup>-1</sup> under an argon atmosphere; DMF and Bu<sub>4</sub>NPF<sub>6</sub> were used without further purification. A solution of Bu<sub>4</sub>NPF<sub>6</sub> was scanned before use to check the purity of the solvent. The reported *E*<sub>1</sub> values were determined from stationary experiments at a rotating electrode (LSV).

#### Preparation of a cobalt(II) croconate, [CoL<sup>1</sup>(H<sub>2</sub>O)<sub>3</sub>] **1**

The compound was obtained according to West<sup>26</sup> by reaction in the dark of dipotassium croconate (K<sub>2</sub>L<sup>1</sup>) and CoCl<sub>2</sub>·6H<sub>2</sub>O in water. The product was recrystallized from water as purple crystals (yield ca. 60%) (Found: C, 23.26; H, 2.22. Calc. for C<sub>5</sub>H<sub>6</sub>CoO<sub>8</sub>: C, 23.73; H, 2.39%).

#### Preparation of a cobalt(II) croconate violet, K<sub>2</sub>[CoL<sub>2</sub>(H<sub>2</sub>O)<sub>2</sub>]**2**·2H<sub>2</sub>O **2**

The compound was obtained by reaction of dipotassium

croconate violet (K<sub>2</sub>L<sup>2</sup>) (0.332 g, 1 mmol) in a water–acetonitrile mixture (50:50 cm<sup>3</sup>) with CoCl<sub>2</sub>·6H<sub>2</sub>O (0.238 g, 1 mmol) dissolved in water (100 cm<sup>3</sup>). The addition of the ligand to the metal salt is accompanied by a color change from pink to red. Suitable red-brown crystals were obtained after standing the solution for a few days under slow evaporation, at room temperature (yield ca. 40%) (Found: C, 37.61; H, 1.10; N, 15.92. Calc. for C<sub>22</sub>H<sub>8</sub>CoN<sub>8</sub>O<sub>10</sub>K<sub>2</sub>: C, 38.77; H, 1.18; N, 16.44%).

#### Crystallography

Crystal data, intensity measurements and structure refinement are summarized in Table 1. For **1** unit-cell parameters and diffracted intensities were measured at 180 K with the scan rotation  $\phi$  mode on a STOE-I.P.D.S. (imaging plate diffraction system) diffractometer equipped with an Oxford cryosystems cooler device. The crystal to detector distance was 80 mm. Mo-K $\alpha$  radiation ( $\lambda$  0.71073 Å) was employed as X-ray source. Numerical absorption corrections were applied to the data.<sup>27</sup> The structure was solved by direct methods (SIR 92)<sup>28</sup> and refined by least-squares procedures on *F<sub>o</sub>*. Hydrogen atoms were located on a difference Fourier map and isotropically refined with an isotropic thermal parameter fixed at 20% higher than those of their connected oxygen atoms. Atomic scattering factors and anomalous dispersion terms are taken from ref. 29. The plot of the molecule together with the labelling scheme are shown in Fig. 1. Selected interatomic distances and angles are listed in Table 2.

For **2** a small crystal was mounted on a glass fiber with RS3000 oil. Graphite monochromatized Cu-K $\alpha$  radiation ( $\lambda$  1.5418 Å) was employed as X-ray source. Unit-cell parameters and diffracted intensities were measured at 200 K with the scan mode  $\omega$ – $2\theta$  on a STOE-STADI 4 diffractometer. The structure was solved by direct methods (MULTAN 87)<sup>30</sup> and refined by XTAL 3.2 program.<sup>31</sup> Absorption corrections by analytical integration<sup>32</sup> were applied to the data. Atomic scattering factors and anomalous dispersion terms are taken from ref. 28. All H atom co-ordinates were refined using *U*<sub>iso</sub> 0.05 Å<sup>2</sup>. The plot of the molecule together with the labelling scheme are shown in Fig. 2 and 3. Selected interatomic distances and angles are listed in Table 2.

CCDC reference number 186/1202.

**Table 2** Selected interatomic distances (Å) and bond angles (°) with estimated standard deviations in parentheses for **1** and **2**

Complex 1				Complex 2			
Metal environment							
Co–O1	2.103(3)	Co–O6	2.025(3)	Co–O1	2.122(3)	K–O1	2.794(3)
Co–O2	2.152(3)	Co–O7	2.111(3)	Co–O2	2.109(3)	K–N4	2.899(4)
Co–O4	2.103(2)	Co–O8	2.082(3)	Co–O4	2.048(3)	K–O5	2.801(3)
				Co–K	3.7314(9)	K–O3	2.888(3)
						K–O2	2.883(3)
O1–Co–O2	80.8(1)			O1–Co–O2	82.2(1)		
O2–Co–O4	171.6(1)			O4–Co–O1	90.0(1)		
O1–Co–O4	90.8(1)			O4–Co–O2	89.1(1)		
O2–Co–O6	90.5(1)			K–Co–O1	132.12(8)		
O4–Co–O6	97.9(1)			K–Co–O2	129.74(7)		
O1–Co–O7	92.1(1)			K–Co–O4	94.23(9)		
O2–Co–O7	94.2(1)						
O4–Co–O7	86.0(1)						
O2–Co–O8	92.97(9)						
O4–Co–O8	86.7(1)						
O6–Co–O8	90.5(1)						
O6–Co–O7	90.7(1)						
Ligands							
O1–C1	1.256(5)	C1–C2	1.437(5)	O1–C1	1.265(5)	C2–C3	1.432(6)
O2–C2	1.259(5)	C1–C5	1.453(5)	O2–C2	1.258(5)	C3–C4	1.470(5)
O3–C3	1.237(5)	C2–C3	1.457(5)	O3–C4	1.227(5)	C3–C6	1.377(6)
O4–C4	1.248(4)	C3–C4	1.481(5)	N1–C7	1.143(6)	C4–C5	1.473(6)
O5–C5	1.256(4)	C4–C5	1.466(5)	N2–C8	1.150(6)	C5–C9	1.379(5)
				N3–C10	1.148(6)	C6–C7	1.429(6)
				N4–C11	1.153(6)	C6–C8	1.426(6)
				C1–C2	1.457(5)	C9–C10	1.440(6)

## Results and discussion

### Chemistry

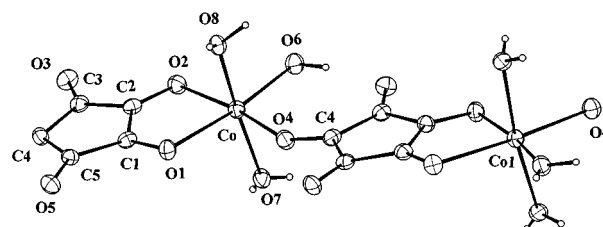
As already mentioned, the cobalt(II)–croconate complex has been obtained according to West and Niu.<sup>26</sup> During their synthesis, they obtained an unidentified pink by-product the analytical data for which fit with the formula of a cobalt–oxalate complex. A few years ago, we reported on the easy photo-oxidation of croconic acid into oxalic and mesoxalic (HO<sub>2</sub>CCOCO<sub>2</sub>H) acids corresponding to croconic ring breaking.<sup>33</sup> So, we think that the pink oxalate complex may result from the same process. To prevent this oxidation, the synthesis of **1** was performed in the dark.

Since the formula of **2** implies two ligands per metallic ion, we attempted to prepare a croconate complex with two ligands using a large excess of croconate ion. In fact, only the complex ML<sup>1</sup>(H<sub>2</sub>O)<sub>3</sub> was obtained.

### Crystal structure of **1**

Preliminary studies on the structure of copper(II), zinc(II) and manganese(II) croconate reveal that although these compounds are isostructural, they are not strictly isomorphous.<sup>5,6</sup> The similarity of the powder diffraction patterns indicates that the croconate complexes of divalent metal ions, nickel(II) and cobalt(II) must have the same structure, although the degree of distortion around the metal ion might vary.

Cobalt(II) croconate consists of infinite chains with an asymmetric repeating unit constituted by one metal, one croconate and three water molecules (Fig. 1). The zig-zag chains are parallel to the *c* axis. Consequently, two neighbouring cobalt(II) ions are separated by a croconate ion with a Co...Co distance of 7.9891(3) Å inside a chain. The close packing involved hydrogen bonds inducing a Co...Co inter-chain distance of 5.0035(6) Å. Each cobalt(II) is co-ordinated to three water molecules, two adjacent oxygen atoms of one croconate ring acting as a chelating ligand (O1 and O2) and a single oxygen (O4) of a second croconate ring. The difference observed between Co–O1 (2.103(3) Å) and Co–O2 (2.152(3) Å)

**Fig. 1** Crystal structure of the complex [CoL<sup>1</sup>(H<sub>2</sub>O)<sub>3</sub>]<sub>n</sub>.

distances confirms the intrinsic tendency of croconate to co-ordinate as an asymmetric bidentate ligand already reflected in the structure of the copper complex; in contrast Co–O4 and Co–O1 distances are comparable. Two of the five oxygen atoms of the croconate ring (O3 and O5) are not metal-co-ordinated. There is no significant difference between the Co–carbonyl and Co–OH<sub>2</sub> bond distances. Analogously, in the croconate ligand, the C–O bond distances for the free or the co-ordinated oxygen atoms are comparable. The average metal–oxygen distance for the cobalt(II) compound is 2.096 Å and the bond anisotropy is much smaller than in the copper(II) complex. The interchain interactions *via* strong hydrogen bonding are analogous to those evidenced for the isostructural metal(II) complexes already described.

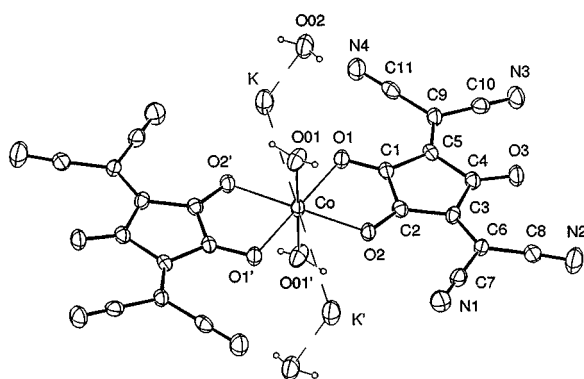
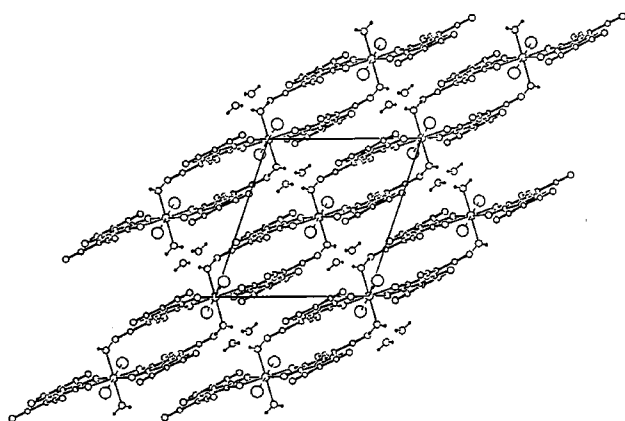
### Crystal structure of **2**

The structure is made of discrete dianionic mononuclear and symmetrical entities of [CoL<sup>2</sup><sub>2</sub>(H<sub>2</sub>O)<sub>2</sub>]<sup>2–</sup> and potassium ions. A plot of the [CoL<sup>2</sup><sub>2</sub>(H<sub>2</sub>O)<sub>2</sub>]<sup>2–</sup> in the structure is presented in Fig. 2. The cobalt atom sits on the inversion centre. It is surrounded by four oxygen atoms of two croconate violet ligands and two water molecules. It is located at the centre of the plane defined by the five ring carbon atoms, the two exocyclic olefinic carbon atoms, and the three oxygen atoms of each ligand. As expected for a cobalt(II) complex, we can observe a tetragonally distorted octahedral geometry with two bond lengths (Co–water) shorter than the four others. Moreover, as underlined in

**Table 3** Hydrogen bonds for complex **2**

Donor–H	Donor...Acceptor	H...Acceptor	Donor–H...Acceptor
O4–H42 0.74(5)	O4...O5 (0) 2.769(5)	H42...O5 (0) 2.04(5)	O4–H42...O5 (0) 169(5)
O4–H41 0.81(5)	O4...N3 (1) 2.866(5)	H41...N3 (1) 2.07(5)	O4–H41...N3 (1) 167(4)
O4–H42 0.74(5)	O4...O2 (2) 2.916(4)	H42...O2 (2) 2.76(5)	O4–H42...O2 (2) 94(4)
O5–H51 0.79(5)	O5...N2 (3) 2.863(6)	H51...N2 (3) 2.18(5)	O5–H51...N2 (3) 144(4)
O5–H52 0.75(5)	O5...O3 (4) 2.813(5)	H52...O3 (4) 2.31(5)	O5–H52...O3 (4) 126(4)

Equivalent positions: (0)  $x, y, z$ ; (1)  $3/2 - x, y - 1/2, 1/2 - z$ ; (2)  $1 - x, 1 - y, 1 - z$ ; (3)  $3/2 - x, 1/2 + y, 1/2 - z$ ; (4)  $1 - x, y, z$ .

**Fig. 2** Crystal structure of the complex  $K_2[CoL_2(H_2O)_2] \cdot 2H_2O$ .**Fig. 3** View of the packing in  $K_2[CoL_2(H_2O)_2] \cdot 2H_2O$  in the  $ac$  plane.

the description of the structure of **1**, the croconate ligand coordinates in an asymmetrical bidentate fashion: in particular, the two Co–O bond distances being 2.122(3) and 2.109(3) Å. The ligand is not strictly planar: the three oxygen atoms and the two methylene carbon atoms lie in the plane of the ring, whereas the two dicyanomethylene groups are rotated, in the same direction, away from the plane of the ring with 4.7° and 5.2° angles. A similar twist of the dicyanomethylene groups out of the ring plane has been observed in the free ligand<sup>16</sup> and in TCNQ.<sup>34,35</sup> In the free ligand,<sup>16</sup> the mean C–C bond length is 1.450 Å lying between 1.437(7) Å (C2–C3) and 1.472(9) Å (C1–C2); in the complex, the mean distance of 1.453 Å is comparable. The carbon ring is not affected by complexation and the values obtained for the C–C bond distances agree with those calculated for the ideal planar geometry. As expected for a delocalized ring, the three C–O bond lengths are identical in the free ligand (average value 1.244 Å) but the complexation

induces a partial localization of the  $\pi$  electrons. This assumption is supported by “the ketonic” bond length of the uncoordinated oxygen atom (1.227(5) Å) compared to the longer C–O bond distances of the oxygen atoms co-ordinated to the cobalt (average value 1.27 Å). It may be underlined that this difference is not evidenced in **1**. Of particular interest are the strong intermolecular hydrogen bonds, Table 3. These involve water molecules and the croconate oxygen O3 which do not participate in complexation evidenced by the O...O distance of 2.813(5) Å and also the nitrogen atoms of the cyano groups. All the oxygen atoms of the ligands are co-ordinated to a potassium atom which is also linked to the crystallisation water molecule.

The sites of co-ordination of either the oxygen or nitrogen of dicyanomethylene groups may be related to a number of parameters: the charge distribution on the oxygen and nitrogen atoms, the soft or hard character of the metal, the geometry of the ligand. In the dicyanomethylene trionate complex **2** the co-ordination occurs only *via* the oxygen atoms. However, we have recently isolated Cu(I) and Cu(II) complexes involving dicyanomethylene pseudo-oxocarbons derived from squaric acid.<sup>1</sup> In these complexes, metal atoms are always co-ordinated by the nitrogen atoms of the dicyanomethylene groups.

### IR and electronic spectroscopies

In **1**, the most relevant IR features are those associated with the chelating croconate. Our spectra are in agreement with the West and Niu analysis.<sup>26</sup> A broad and intense absorption in the 3400–3000  $cm^{-1}$  range is attributed to the OH stretching frequency of the water molecules. Bands at 1740 and 1724  $cm^{-1}$  are assigned to the unco-ordinated carbonyl groups which exhibit a strong double-bond character. The co-ordinated CO groups are characterized by medium absorptions at 1682 and 1660  $cm^{-1}$ . A very strong and broad peak centered at 1500  $cm^{-1}$  is attributed to vibrational modes representing mixtures of C–O and C–C stretching motions. This absorption is characteristic of the salts of  $C_nO_n^{2-}$  ions.<sup>36</sup>

The vibrational spectrum of croconate violet has been analyzed by Fatiadi.<sup>13–17</sup> It shows a band at 2198  $cm^{-1}$  attributed to  $\nu(CN)$  stretching frequencies. In **2**, this vibration, observed at 2208  $cm^{-1}$ , is slightly shifted and confirms that the nitrile groups are not engaged in the complexation with Co. Moreover, the band at 1674  $cm^{-1}$  in the free ligand, attributed by Fatiadi to the carbonyl groups, completely disappears in the cobalt complex, even though one of the ring carbonyl groups remains free and is not implicated in the co-ordination. In the group of bands at 1615, 1572 and 1521  $cm^{-1}$  the problem of the vibrational assignments appeared as difficult due to the strong coupling of the C=O oscillators and to the C=O and C=C coupling. In the complex these bands are not significantly



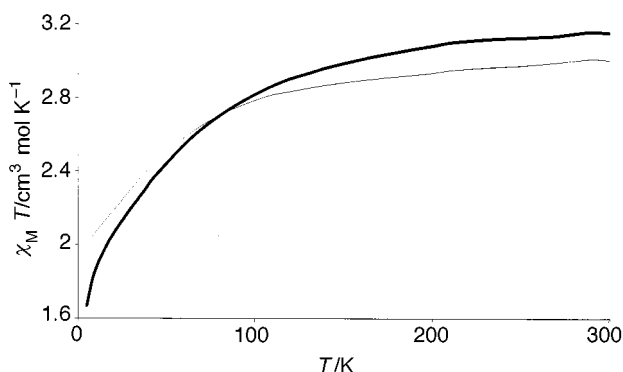


**Fig. 4** Temperature dependence of  $\chi_M T$  for  $[\text{CoL}(\text{H}_2\text{O})_3]_n$  (—) and  $\text{K}_2[\text{CoL}_2(\text{H}_2\text{O})_2] \cdot 2\text{H}_2\text{O}$  (---).

shifted by complexation and remain practically unchanged (1609, 1562 and  $1515\text{ cm}^{-1}$ ).

Owing to their strong absorption in the visible spectrum, the croconate dyes have been investigated for their photophysical properties.<sup>37</sup> In DMF, croconate ion is yellow and displays a characteristic absorption at 334 nm ( $\epsilon = 24000\text{ L mol}^{-1}\text{ cm}^{-1}$ ) and croconate violet is a dye characterized by a strong absorption in the visible spectrum at 534 nm ( $\epsilon = 88000\text{ L mol}^{-1}\text{ cm}^{-1}$ ). As concerns the cobalt complexes, high-spin six-co-ordinated octahedral or pseudo-octahedral cobalt(II) species will exhibit three allowed transitions.<sup>38</sup> However,  $\nu^1$  corresponding to the  ${}^4\text{T}_{1g} \rightarrow {}^4\text{T}_{2g}$  transition was not observed within the wavelength sweep from UV to near IR. The other transitions are hidden by the absorption bands of the ligands. The UV/VIS spectra of the cobalt complexes present the same pattern as the ligands (complex **1**, 328 nm ( $\epsilon = 21500\text{ L mol}^{-1}\text{ cm}^{-1}$ ) and complex **2**, 532 nm ( $\epsilon = 66000\text{ L mol}^{-1}\text{ cm}^{-1}$ )).

### Magnetic properties

Most six-co-ordinated cobalt(II) complexes fall into two classes: those with magnetic moments which lie in the range  $4.8\text{--}5.6\ \mu_B$  and are referred to as “high-spin” and those with moments in the range  $1.73\text{--}2.0\ \mu_B$  which are referred to as “low-spin”. However, there has been found between these two classes a number of six-co-ordinated cobalt(II) compounds which have intermediate magnetic moments at room or lower temperatures. These thermally induced spin conversions  $S = 3/2 \leftrightarrow S = 1/2$  were generally found to be gradual, often extending over more than 100 K.<sup>39–41</sup>

The ground state of the free Co(II) ion is  ${}^4\text{F}$ , but the orbital degeneracy is removed in an octahedral crystal field giving one  ${}^4\text{A}$  and two  ${}^4\text{T}$  levels with the lowest-lying state being  ${}^4\text{T}_{1g}$ .<sup>38</sup> The temperature dependence of the product  $\chi_M T$  ( $\chi_M$  denoting the molar magnetic susceptibility) for the complexes **1** and **2** is plotted in Fig. 4. The  $\chi_M T$  values ( $\chi_M T = 3.006\text{ cm}^3\text{ mol}^{-1}\text{ K}$ ,  $\mu_{\text{eff}} = 4.90\ \mu_B$ ) obtained at 300 K for **2** with a continuous decrease upon cooling are typical of cobalt(II) high-spin species. At 4 K, the  $\mu_{\text{eff}}$  for **2** lies in the range expected for high-spin cobalt(II) ( $\mu_{\text{eff}} = 4.00\ \mu_B$ ). In light of crystallographic measurements, it is clear that there is a distortion from octahedral symmetry in **2**. However, the poor distortion value ( $0.05\text{ \AA}$ ) indicates that only the spin–orbit coupling has to be taken into account and that Jahn–Teller stabilization is small as expected.<sup>42</sup>

Recent reports on magnetic studies of some chain and layered six-co-ordinated cobalt(II) compounds show<sup>43</sup> that, at low temperature, these magnetic systems behave as collections of Ising chain  $S = 1/2$  effective spins coupled usually by ferromagnetic<sup>44–46</sup> but also antiferromagnetic interactions.<sup>47</sup> For such species, the degeneracy of the  ${}^4\text{T}_{1g}$  ground triplet is removed by the combined action of spin–orbit coupling and axial or rhombic distortions of the crystal field, giving six Kramers doublets with an effective nonisotropic  $S = 1/2$  ground state.

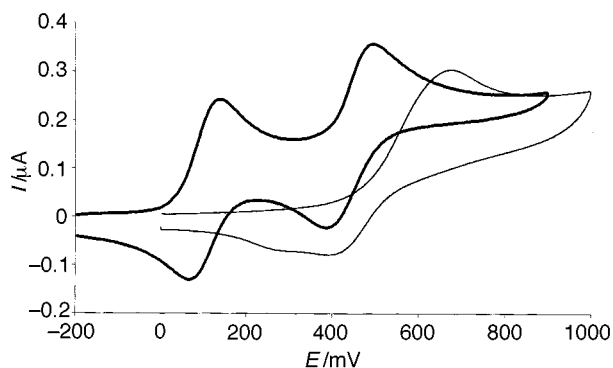
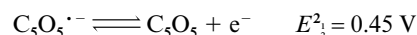
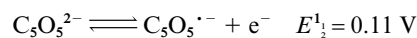


**Fig. 5** Cyclic voltammograms at a Pt disc electrode (diameter 0.5 mm) in DMF– $\text{Bu}_4\text{NPF}_6$   $0.1\text{ mol L}^{-1}$ :  $[\text{PPh}_4]_2\text{C}_5\text{O}_5$ ,  $1.2\text{ mmol L}^{-1}$  (—); complex **1**,  $1\text{ mmol L}^{-1}$  (---); potential scan speed  $0.1\text{ V s}^{-1}$ , potentials are measured *versus* SCE.

For complex **1**,  $\chi_M T = 3.15\text{ cm}^3\text{ mol}^{-1}\text{ K}$  ( $\mu_{\text{eff}} = 5.02\ \mu_B$ ) at 300 K and  $1.67\text{ cm}^3\text{ mol}^{-1}\text{ K}$  ( $\mu_{\text{eff}} = 3.65\ \mu_B$ ) at 4 K. This last value is lower than the spin-only value for a high-spin cobalt(II) complex but far from the value generally observed at low temperature for a Ising  $S = 1/2$  chain ( $\mu_{\text{eff}} = 2.0\ \mu_B$ ). A possible interpretation of our experimental results requires that a proportion of cobalt(II) is in the low-spin form at low temperature. Another interpretation is to involve exchange antiferromagnetic interactions between the paramagnetic centres. Magnetic properties of isostructural croconate complexes have been investigated in the past few years and magnetic exchanges have been evidenced.<sup>6,7</sup> For manganese(II) croconate complexes two studies have been performed. In the first, in our own work,<sup>8</sup> we suggested that spin–spin interactions are likely to occur between manganese ions of neighbouring chains. In the second, Gatteschi *et al.*<sup>7</sup> neglects interchain interactions favouring a weak antiferromagnetic coupling between the spins *via* the croconate ligand ( $J = 0.22\text{ cm}^{-1}$ ). However, it may be underlined that some values, slightly lower than the spin-only value, have been observed in mononuclear complexes which do not exhibit any spin transition, deviations at the spin-only value being accounted for by axial distortion of the cobalt(II) octahedral environment.<sup>38,41</sup>

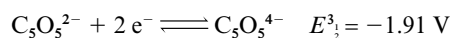
### Redox properties

**Complex 1.** In organic solvents, the electrochemical oxidation of the croconate dianion is well known.<sup>18,33</sup> Under non-stationary conditions at a Pt electrode, the voltammogram shows two oxidation waves (Fig. 5) which appear mono-electronic and reversible. The oxidation process is expressed by two successive electron transfers with a high electron transfer rate:



The orange radical anion  $\text{C}_5\text{O}_5^{\cdot-}$  is very stable (few hours). Its potential domain ( $E_2^\circ - E_1^\circ$ ) depends on the solvent:  $0.53\text{ V}$  in  $\text{CH}_3\text{CN}$  and  $0.34\text{ V}$  in DMF. The radical anion  $\text{C}_5\text{O}_5^{\cdot-}$  is less stable in DMF than in  $\text{CH}_3\text{CN}$ .

Moreover, a reduction process is observed around  $-1.9\text{ V}$ . Under slow potential scan speed the process is irreversible and the peak current is twice that of the oxidation peak. By increasing the potential scan speed at a  $50\text{ }\mu\text{m}$  Pt electrode, the reduction process appeared reversible (in the range  $100\text{ V s}^{-1}$  up to  $2500\text{ V s}^{-1}$ ). Taking into account the results, the reduction process may be expressed by:



In the electroactivity domain of DMF, the cyclic voltammogram of **1** is restricted to an oxidation process (Fig. 5). At a

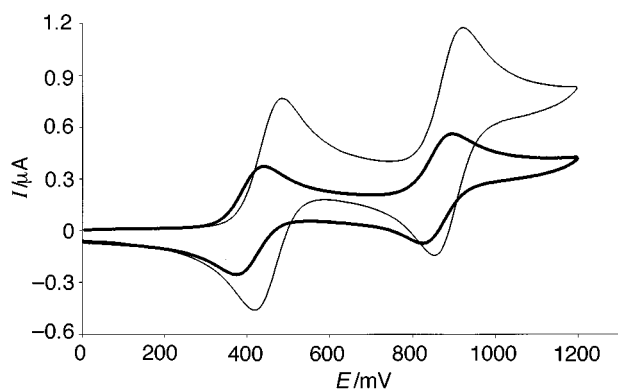
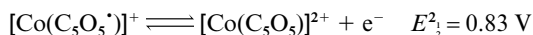
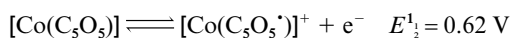


**Fig. 6** Cyclic voltammograms at a Pt disc electrode (diameter 0.5 mm) in DMF–Bu<sub>4</sub>NPF<sub>6</sub> 0.1 mol L<sup>-1</sup>; K<sub>2</sub>L<sup>2</sup> 1 mmol L<sup>-1</sup>; (—); complex **2** 1 mmol L<sup>-1</sup> (---); potential scan speed 0.1 V s<sup>-1</sup>, potentials are measured *versus* SCE.

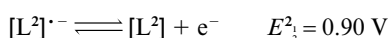
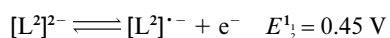
rotating disc electrode, two nearly equal waves were observed with  $E_1^1 = 0.62$  V and  $E_2^1 = 0.83$  V. The pattern of the cyclic voltammogram (Fig. 5) shows that the process is complex. According to the variations of the voltammograms as a function of the potential scan speed, the process may be classified as a bielectronic process with close potentials. In fact, this electrochemical process matches the oxidation of the C<sub>5</sub>O<sub>5</sub><sup>2-</sup> ligand. In Fig. 5, the mean oxidation peak current of **1** is nearly the sum of the oxidation peak currents of free C<sub>5</sub>O<sub>5</sub><sup>2-</sup>. Owing to complexation, the potentials  $E_1^1$  and  $E_2^1$  are shifted towards anodic potentials and get close together:



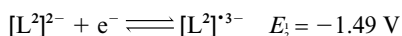
Simulation curves with the Gosser program<sup>48</sup> gave an approximation of the electrooxidation mechanism. It can be assumed to be two electron transfers with slow electron transfer rates which are coupled to chemical reactions such as the decomplexation of the radical complex. As a consequence, the potential domain of the radical anion C<sub>5</sub>O<sub>5</sub><sup>·-</sup> is reduced and the bound C<sub>5</sub>O<sub>5</sub><sup>·-</sup> is unstable. Such a case was already observed in the study of platinum complexes with squarate and croconate dianions: the electrochemical measurements did not show the radical anion step.<sup>49</sup> According to the potential displacement as a function of complexation,<sup>50</sup> the positive shift of the redox potentials of C<sub>5</sub>O<sub>5</sub><sup>2-</sup> shows that the complex formation constants of the C<sub>5</sub>O<sub>5</sub><sup>·-</sup> radical anion and the neutral C<sub>5</sub>O<sub>5</sub> are lower than the one of the C<sub>5</sub>O<sub>5</sub><sup>2-</sup> dianion.

In the cathodic domain, the reduction of the C<sub>5</sub>O<sub>5</sub><sup>2-</sup> dianion in the complex was not observed. This is in agreement with the decrease of the co-ordination properties of the C<sub>5</sub>O<sub>5</sub><sup>2-</sup> dianion upon oxidation or reduction.

**Complex 2.** The electrochemical oxidation of croconate violet ([L<sup>2</sup>]<sup>2-</sup>) has already been reported.<sup>18</sup> Under non stationary conditions at a Pt electrode, the voltammogram shows two oxidation waves (Fig. 6) that appear monoelectronic and reversible. The oxidation process is expressed by the two successive electron transfers with high electron transfer rate:

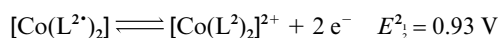
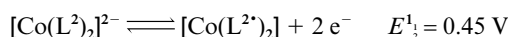


Moreover, a monoelectronic reduction process is observed at  $E_2 = -1.49$  V which also appears reversible (quasi reversible in CH<sub>3</sub>CN,  $E_2 = -1.53$  V):



The radical anion [L<sup>2</sup>]<sup>·-</sup> is very stable. Its potential domain ( $E_2^1 - E_1^1$ ) depends on the solvent: 0.66 V in CH<sub>3</sub>CN and 0.45 V in DMF. The radical anion [L<sup>2</sup>]<sup>·-</sup> is less stable in DMF than in CH<sub>3</sub>CN. On the contrary, the radical trianion [L<sup>2</sup>]<sup>· 3-</sup> is only stable over the time scale of the cyclic voltammetry. By comparison of the voltammograms of the C<sub>5</sub>O<sub>5</sub><sup>2-</sup> dianion (Fig. 5) and the [L<sup>2</sup>]<sup>2-</sup> dianion (Fig. 6), it is observed that the dicyanomethylene groups shift the redox potentials towards anodic potentials.

In the electroactivity domain of DMF, the cyclic voltammogram of **2** presents the same oxidation process as the free ligand (Fig. 6). The reduction process of the ligand is not present in the complex. The electrochemical study was restricted to the oxidation processes. Under stationary conditions, at a Pt disc electrode (Fig. 6), the voltammogram of the complex presents two oxidation waves: a first oxidation wave with  $E_1^1 = 0.45$  V and a second one with  $E_2^1 = 0.93$  V. These values match the potentials of the free ligand oxidation (0.45 V and 0.90 V). Furthermore, the comparison between the peak current intensities in Fig. 6 shows that while the free ligand oxidation proceeds through two successive monoelectronic transfers, the oxidation of **2** proceeds through two bielectronic transfers (the oxidation of the two [L<sup>2</sup>]<sup>2-</sup> ligands). Taking into account the Randles–Sevcik equation in which the peak current is related to  $n^{3/2}$ , number of transferred electrons, it appears that the oxidations of the two [L<sup>2</sup>]<sup>2-</sup> ligands are independent. This may be expressed by:



According to the potential displacement as a function of complexation<sup>50</sup> and taking into account the disappearance of the reduction peak of the free ligand ( $E_2 = -1.49$  V) on the voltammogram of **2**, it can be postulated that the complex is not dissociated in DMF. This was confirmed by conductimetric measurements. Furthermore, the invariability of the redox potentials of the oxidations shows that the formation constants of Co(II) with [L<sup>2</sup>]<sup>2-</sup>, [L<sup>2</sup>]<sup>·-</sup> or L<sup>2</sup> species are of the same order of magnitude. This is in favour of the contribution of the dicyanomethylene groups in the stabilization of the charge. In particular, the radical would be localized on the dicyanomethylene group as in the 3,4-bis(dicyanomethylene)cyclobutane-1,2-dione radical anion.<sup>51</sup>

Finally, the electrochemical behaviour at a Pt electrode of complexes **1** and **2** is limited to the oxidation of the ligands. No reduction or oxidation of Co(II) was observed. The disappearance of the electrochemical reduction of the ligands in the complexes confirmed their complexation in solution. Moreover, the electrochemical behaviours of complexes **1** and **2** are quite different. In complex **2**, the oxidation process corresponds to the oxidation of two independent [L<sup>2</sup>]<sup>2-</sup> ligands while in complex **1** the oxidation of the C<sub>5</sub>O<sub>5</sub><sup>2-</sup> dianions is perturbed by Co(II) complexation. If the introduction of dicyanomethylene groups shifts the oxidation potentials towards anodic potentials, it also increases the potential domain of the radical (0.34 V to 0.45 V in the free ligands and 0.21 V to 0.48 V in the complexes). The positive shift of the oxidation potentials is in agreement with the polarographic data of quinones and dicyanomethylene substituted quinones.<sup>52</sup> But in this latter case the potential domain of the “semiquinone” radical is decreased. However, this radical stabilization is encouraging for the synthesis and characterization of metal–radical ligand complexes.

## Acknowledgements

We gratefully acknowledge A. Mari, Laboratoire de Chimie de Coordination du CNRS, Toulouse, for technical assistance with magnetic measurements.

## References

- 1 Part 1. C. Pena, A. M. Galibert, B. Soula, P. L. Fabre, G. Bernardinelli and P. Castan, *J. Chem. Soc., Dalton Trans.*, 1998, 239.
- 2 L. Gmelin, *Ann. Phys. (Leipzig)*, 1825, 431.
- 3 L. Gmelin, *Justus Liebigs Ann. Chem.*, 1841, **37**, 58.
- 4 S. Cohen, J. R. Lacher and J. D. Park, *J. Am. Chem. Soc.*, 1959, **81**, 3480.
- 5 M. D. Glick, G. L. Downs and L. F. Dahl, *Inorg. Chem.*, 1964, **3**, 1712.
- 6 M. D. Glick and L. F. Dahl, *Inorg. Chem.*, 1966, **5**, 289.
- 7 A. Cornia, A. C. Fabretti, A. Giusti, F. Ferraro and D. Gatteschi, *Inorg. Chim. Acta*, 1993, **212**, 87.
- 8 D. Deguenon, G. Bernardinelli, J. P. Tuchagues and P. Castan, *Inorg. Chem.*, 1990, **29**, 3031.
- 9 P. Castan, D. Deguenon and F. Dahan, *Acta Crystallogr., Sect. A*, 1991, **47**, 2656.
- 10 I. Castro, J. Sletten, J. Faus and M. Julve, *J. Chem. Soc., Dalton Trans.*, 1992, 2271.
- 11 I. Castro, J. Sletten, J. Faus, M. Julve, Y. Journaux, F. Lloret and S. Alvarez, *Inorg. Chem.*, 1992, **31**, 1889.
- 12 R. West, *Oxocarbons*, Academic Press, New York, 1980.
- 13 A. J. Fatiadi, *J. Am. Chem. Soc.*, 1978, **100**, 2586.
- 14 A. J. Fatiadi, *Synthesis*, 1978, **3**, 165.
- 15 A. J. Fatiadi, *J. Org. Chem.*, 1980, **45**, 1338.
- 16 V. L. Himes, A. D. Mighell, C. R. Hubbard and A. Fatiadi, *J. Res. Natl. Bur. Stand. (US)*, 1980, **85**, 87.
- 17 A. J. Fatiadi, *Oxocarbons*, Academic Press, New York, 1980.
- 18 L. M. Doane and A. J. Fatiadi, *J. Electroanal. Chem. Interfacial Electrochem.*, 1982, **135**, 193.
- 19 P. V. Kamat and M. A. Fox, *J. Electroanal. Chem. Interfacial Electrochem.*, 1983, **159**, 49.
- 20 P. V. Kamat and M. A. Fox, *Chem. Phys. Lett.*, 1982, **92**, 595.
- 21 P. V. Kamat, M. A. Fox and A. J. Fatiadi, *J. Am. Chem. Soc.*, 1984, **106**, 1191.
- 22 N. Venkatalakshmi, B. Varghese, S. Lalitha, R. F. X. Williams and P. T. Manoharan, *J. Am. Chem. Soc.*, 1989, **111**, 5748.
- 23 W. B. Heuer and W. H. Pearson, *J. Chem. Soc., Dalton Trans.*, 1996, 3507.
- 24 A. Fatiadi, H. S. Isbell and W. F. Sager, *J. Res. Natl. Bur. Stand., Sect. A*, 1963, **67**, 153.
- 25 P. W. Selwood, *Magnetochemistry*, Interscience, New York, 1956.
- 26 R. West and H. Y. Niu, *J. Am. Chem. Soc.*, 1963, **85**, 2586.
- 27 X-Shape, a program for numerical Absorption correction (version 1.01), STOE and Cie, GMBH, Darmstadt, Germany, 1996.
- 28 A. Altomare, G. Carasciano, G. Giacovazzo, A. Guagliardi, M. C. Burla, G. Polidori and M. Camalli, *J. Appl. Crystallogr.*, 1994, **27**, 435.
- 29 *International Tables for X-Ray Crystallography*, Kynoch Press, Birmingham, 1974, vol.4.
- 30 P. Main, S. J. Fiske, S. E. Hull, L. Lessinger, G. Germain, J. P. Declercq and M. M. Woolfson, *MULTAN 87*, A system of Computer Programs for the Automatic Solution of Crystal Structures from X-Ray Diffraction Data, Universities of York and Louvain-la-Neuve, 1987.
- 31 S. R. Hall and J. M. Steward (Editors), *XTAL3.2 Users Manual*, Universities of Western Australia and Maryland, 1992.
- 32 E. Blanc, D. Schwaezenbach and H. D. Flack, *J. Appl. Crystallogr.*, 1991, **24**, 1035.
- 33 P. L. Fabre, P. Castan, D. Deguenon and N. Paillous, *Can. J. Chem.*, 1995, **73**, 129.
- 34 T. J. Kistenmacher, T. E. Phillips, D. O. Cowan, J. P. Ferraris, A. N. Bloch and T. O. Poehler, *Acta Crystallogr., Sect. B*, 1976, **32**, 539.
- 35 T. J. Kistenmacher, T. E. Phillips and D. O. Cowan, *Acta Crystallogr., Sect. B*, 1974, **30**, 763.
- 36 M. Ito and R. West, *J. Am. Chem. Soc.*, 1963, **85**, 2580.
- 37 P. V. Kamat and M. A. Fox, *J. Photochem.*, 1984, **24**, 285.
- 38 L. Banci, A. Bencini, C. Benelli, D. Gatteschi and C. Zanchini, *Struct. Bonding (Berlin)*, 1982, **52**, 37.
- 39 J. Zarenbowitch, R. Claude and O. Kahn, *Inorg. Chem.*, 1985, **24**, 1576.
- 40 J. Zarenbowitch, R. Claude and P. Thuery, *New. J. Chem.*, 1985, **9**, 467.
- 41 J. Zarenbowitch and O. Kahn, *Inorg. Chem.*, 1984, **23**, 589 and refs. therein.
- 42 F. S. Ham, *Phys. Rev.*, 1965, **138**, 1727.
- 43 W. E. Hatfield, W. E. Estes, W. E. Marsh, M. W. Pickens, L. W. Ter Haar and R. R. Weller, in *Extended Linear Chain Compounds*, ed. J. S. Miller, Plenum Press, New York and London, vol. 3, p. 43.
- 44 S. Angelov, M. Drillon, E. Zhecheva, R. Stoyanova, M. Belaiche, A. Derory and A. Herr, *Inorg. Chem.*, 1992, **31**, 1514.
- 45 W. Zhang, C. P. Landee, M. M. Turnbull and R. D. Willett, *J. Appl. Phys.*, 1993, **73**, 5379.
- 46 W. Zhang, J. R. Jeitler, M. M. Turnbull, C. P. Landee, M. Wei and R. D. Willett, *Inorg. Chim. Acta*, 1997, **256**, 183.
- 47 G. De Munno, T. Poerio, M. Julve, F. Lloret and G. Viau, *New J. Chem.*, 1998, 299.
- 48 D. K. Gosser, *Cyclic Voltammetry Simulation and Analysis of Reaction Mechanisms*, VCH, New York, 1993.
- 49 P. Castan, D. Deguenon, P. L. Fabre and G. Bernardinelli, *Polyhedron*, 1992, **11**, 901.
- 50 B. Trémillon, *Electrochimie analytique et réactions en solution*, Masson, Paris, vol. 2, 1993.
- 51 G. Farnia, B. Lunelli, F. Marcuzzi and G. Sandona, *J. Electroanal. Chem. Interfacial Electrochem.*, 1996, **404**, 261.
- 52 K. Wallenfels, K. Friedrich, J. Rieser, W. Ertel and H. K. Thieme, *Angew. Chem., Int. Ed. Engl.*, 1976, **15**, 261.

Paper 8/07687A